Russian Journal of Earth Sciences Online ISSN: 1681-1208

Special Issue: "Kamchatka Earthquake M 8.8 on July 29, 2025"

Centroid Moment Tensor of the Kamchatka Earthquake on July 29, 2025 Determined on GNSS Data and ISOLA Software Package

D. A. Safonov[1,*], N. V. Shestakov[2,3], V. V. Pupatenko[4], and A. S. Prytkov[1]

[1] Institute of Marine Geology and Geophysics FEB RAS, Yuzhno-Sakhalinsk, Russian Federation
[2] Far Eastern Federal University, Vladivostok, Russian Federation
[3] Institute of Applied Mathematics FEB RAS, Vladivostok, Russian Federation
[4] Institute of Tectonics and Geophysics FEB RAS, Khabarovsk, Russian Federation
* **Correspondence to:** D. A. Safonov, d.safonov@imgg.ru

Abstract: Using the example of the Kamchatka earthquake on July 29, 2025, this study demonstrates the ability to determine the centroid moment tensor (CMT) of a strong earthquake based on GNSS records at regional distances. We used the ISOLA software package, which is typically used to obtain CMT solutions for weaker earthquakes. The CMT solution obtained using GNSS data agrees well with the solutions from leading global seismological agencies that used seismic records at teleseismic distances. It is also comparable to the CMT solution obtained by the authors based on seismic data from regional seismic stations. Due to the wide selection of GNSS observation point displacement records, which significantly exceeds the number of seismic observation points with broadband equipment, it was possible to obtain a better centroid location. The fact that there are no restrictions on the lower frequencies of the earthquake wave spectrum in GNSS records allowed us to determine the magnitude of the Kamchatka earthquake with high accuracy. The use of GNSS records in conjunction with traditional seismological data can be recommended for inclusion into the procedures of seismological services responsible for registering largest regional earthquakes and warning the population in hazardous areas of the threat of a tsunami.

Keywords: Strong earthquake, focal mechanism solution, centroid moment tensor inversion, global navigation satellite systems, scalar seismic moment, Kamchatka megathrust earthquake

Citation: Safonov D. A., Shestakov N. V., Pupatenko V. V., and Prytkov A. S. (2026), Centroid Moment Tensor of the Kamchatka Earthquake on July 29, 2025 Determined on GNSS Data and ISOLA Software Package, *Russian Journal of Earth Sciences*, 26, ES2015, EDN: ULOMVG, https://doi.org/10.2205/2026es001125

Research Article

Received: February 2, 2026
Accepted: May 25, 2026
Published: July 1, 2026

1. Introduction

The centroid moment tensor (CMT) contains information about the orientation of the fault plane, the direction and scale of displacement at the earthquake's focus. The CMT parameters are determined by inversion of the Earth's surface displacement records.

To determine the CMT for strong and moderately strong events, broadband velocimeter records are used, typically from large regional or global networks such as GSN [*Davis*, 2024]. The most authoritative global and regional agencies are GlobalCMT [*Dziewonski et al.*, 1981; *Ekström et al.*, 2012], USGS [*Hayes et al.*, 2009]; GFZ (GEOFON) [*Quinteros et al.*, 2021]; IPGP (GEOSCOPE) [*Vallée and Douet*, 2016]; and NIED [*Kubo et al.*, 2002]. In Russia, regular CMT catalogs are published by the Geophysical Survey of the Russian Academy of Sciences [*Abubakirov et al.*, 2025] based on data from the Kamchatka [*Abubakirov and Pavlov*, 2021] and Sakhalin [*Safonov and Konovalov*, 2017] branches.

Over recent decades, the role of high-rate (1 Hz and above) continuous GNSS (Global Navigation Satellite System) stations has grown significantly in seismology, including

for CMT estimation. GNSS is used for rapid inversion of point and extended sources. These data have made it possible to determine or improve the model of the foci of many earthquakes, beginning with the Tohoku megathrust earthquake (M_W = 9.0) [*Gusman et al.*, 2012]. Works [*Käufl et al.*, 2014; *Melgar et al.*, 2012; *O'Toole et al.*, 2012; *Riquelme et al.*, 2016; *Zheng et al.*, 2012] can be cited as examples of the successful implementation of GNSS. GNSS plays a role in predicting tsunami wave propagation, thanks to the ability to rapidly estimate the magnitude of a potentially tsunamigenic event [*Crowell et al.*, 2013; *Melgar et al.*, 2015], as well as to obtain a basic model of the focal displacement.

GNSS observation records have several advantages over traditional broadband velocigraphs and accelerographs: no clipping; availability of the lowest frequencies; direct measurement of surface displacements, removing the necessity of signal integration; and no need for "classical" deconvolution.

The main limitation of using GNSS in seismology is the "lower sensitivity threshold": when $M_W < 6.0$, the co-seismic displacements become smaller than the instrumental noise level of the GNSS. Modern high-frequency GNSS records, after careful processing, have an accuracy of about 5–10 mm in the horizontal plane and 20–30 mm in the vertical plane. In real-time regime, in most cases, the achievable accuracy is at least twice as poor, with the exception of the VADASE method [*Colosimo et al.*, 2011].

Since 2012, the Institute of Marine Geology and Geophysics of the Far Eastern Branch of the Russian Academy of Sciences, and the Sakhalin Branch of the Federal Research Center "Geophysical Survey of the Russian Academy of Sciences" [*Safonov and Konovalov*, 2017; *Safonov et al.*, 2015] have been using the ISOLA (ISOLated Asperities) software package [*Sokos and Zahradnik*, 2013; *Sokos and Zahradnik*, 2008; *Zahradnik et al.*, 2005] to determine the CMT of strong and moderately strong earthquakes (M = 4.0–7.5) in the Russian Far East.

The earthquake on July 29, 2025, at 23:24 UTC, with a magnitude of 8.8 and an epicenter off the eastern coast of Kamchatka, technically goes beyond the range of events typically dealt with by ISOLA. Modern methods using the W-phase [*Riquelme et al.*, 2016] or finite fault modeling and inversion are better suited for a detailed study of such an extended source, but they are more complex to configure and less suitable for the rapid, automatic determination of earthquake source parameters.

The objective of this study is to assess the possibility of using GNSS records to determine the CMT of strong, potentially tsunamigenic earthquakes with ISOLA, based on the example of the earthquake that occurred on July 29, 2025, at 23:24 UTC, M_W = 8.8.

To estimate the accuracy of the results, we used the CMT solution for this event obtained using ISOLA but based on broadband seismometer records, as well as CMT solutions for this event from the leading global seismological agencies.

2. Materials and Methods

The initial CMT of the Kamchatka earthquake was obtained using regional and nearest teleseismic broadband velocimeter records. The objective was to obtain the solution based on records from the nearest seismological observation points outside the "near-field" zone. However, all broadband records from seismic stations located more than 1000 km away were found to be clipped. The use of observation points that were too distant was not considered, so that the standard methodological approach and regional velocity profile, which had been tested on weaker earthquakes, could still be applied.

The selection of seismic records for inversion was significantly influenced by the frequency range of broadband velocimeters utilized at diverse seismic stations. The flat section of the amplitude-frequency response of the most common broadband velocimeters in the Far East, Guralp CMG-3 and Streckeisen STS-2, ends at approximately 0.008 Hz. This frequency proved to be insufficient for obtaining a high-quality CMT solution of the source of the seismic event under consideration. A stable solution can be obtained using these sensors; however, the filtering bandwidth at which the solution can be stabilized could not be lowered below 0.005–0.009 Hz. At such settings of the algorithm the solution turns out

to be different from the ones given in Table 1 variants according to the data of authoritative international agencies. Additionally, the seismic moment has been underestimated; the moment magnitude of the event ranges from M_W = 8.5–8.6, i.e., significantly lower than the accepted value of M_W = 8.8 for the event.

Table 1. Parameters of CMT solution of the Kamchatka earthquake on July 29, 2025.

Agency	Lat, °N	Lon, °E	Depth, km	M_W	M_0, Hm	Strike	Dip	Rake
GCMT*	50.36	158.23	36.3	8.7	1.58E+22	214	18	84
USGS**	52.50	160.24	21.5	8.83	2.22E+22	198	18	51
GFZ***	52.54	160.10	20	8.8	1.90E+22	209	13	73
IPGP****	52.47	160.40	31	8.75	1.66E+22	232	19	16
ISOLA-s	51.84	159.64	30	8.8	2.02E+22	203	16	69
ISOLA-g	49.79	157.57	30	8.81	2.06E+22	208	17	65

Notes: *https://www.globalcmt.org Event ID 202507292324B;
**https://earthquake.usgs.gov/earthquakes/eventpage/us6000qw60/moment-tensor;
***https://geofon.gfz.de/eqinfo/event.php?id=gfz2025otqm;
****https://geoscope.ipgp.fr/index.php/en/catalog/earthquake-description?seis=us6000qw60.

It was decided to include only Streckeisen STS-1 sensors, which operate at low frequencies down to 0.003 Hz, in the search for a CMT solution; such sensors are still in operation at the eight nearest seismic stations, and a usable signal was successfully obtained within the 0.002–0.005 Hz filtering range.

Records of seismic stations of the SB FRC GS RAS [*Kostylev*, 2021] were used: YSS and KHBR, the F-net network of the NIED agency [*Kubo et al.*, 2002] URH, HSS, TMR. The nearest GSN points available through Wilber-3 service [*Trabant et al.*, 2012] are also involved: MDJ, HIA, INCN (Table 2). The epicentral distances of the involved observing points range from 1400 to 3100 km, which slightly exceeds the typical regional distances for ISOLA. The azimuthal coverage of the used points turned out to be rather narrow – all stations are located to the southwest of the earthquake epicenter. This usually has a negative effect on the accuracy of the centroid position in space, but the quality of the seismic moment tensor is less significantly affected.

Table 2. Parameters of seismological registration points used in the search for CMT solution of the Kamchatka earthquake on July 29, 2025.

	Installation point	Code	Lat, °N	Lon, °E	Azimuth, °	Distance, km
1	Yuzhno-Sakhalinsk	YSS	46.960	142.760	251	1407
2	Urahoro	URH	42.930	143.671	236	1637
3	Sapporo	HSS	42.967	141.229	241	1776
4	Khabarovsk	KHBR	48.473	135.051	266	1841
5	Tomari	TMR	41.102	141.383	236	1915
6	Mudanjiang	MDJ	44.620	129.590	261	2413
7	Hailar	HIA	49.270	119.741	279	2843
8	Incheon	INCN	37.478	126.624	251	3099

Of the more than a hundred available GNSS equipment installation sites in the Far East of the Russian Federation, twenty were preliminarily selected. The selection was based on the following criteria: proximity to the epicenter but outside the "near-field" zone, which is defined by gradually rejecting nearby points; good recording quality; azimuthal coverage; and avoiding densification of points, as the value of several records from one area is minimal. After removing records that did not meet the minimum quality requirements or were critically inconsistent with the others, 11 GNSS points remained. Unfortunately, GNSS stations from the northern part of Kamchatka had to be excluded. Thus, the azimuthal coverage of the focal area remained modest, though better than the ISOLA solution based on seismic station records.

The ISOLA algorithm recommends a minimum of nine waveforms for inversion: three observation points, each with three channels (NS, EW, and Z). This ensures that the selected data are sufficiently excessive.

Table 3. Parameters of GNSS recording points used in the search for CMT solution of the Kamchatka earthquake on July 29, 2025.

	Installation point	Code	Lat, °N	Lon, °E	Azimuth, °	Distance, km
1	Okha*	OKHB	53.602	142.946	289	1172
2	Nogliki**	NGLK	51.811	143.156	273	1178
3	Kurilsk*	ITUR	45.231	147.873	233	1220
4	Tymovskoje*	TYMV	50.865	142.675	269	1234
5	Onor**	ONOR	50.188	142.669	265	1257
6	Uglegorsk*	UGLG	49.076	142.065	261	1342
7	Yuzhno-Sakhalinsk**	USH1	46.973	142.695	251	1407
8	Anadyr**	ADR1	64.734	177.513	29	1675
9	Khabarovsk**	KHAB	48.495	135.050	266	1841
10	Amga**	AMGA	60.896	131.981	310	1952
11	Vladivostok**	VLD1	43.119	131.890	255	2354

Notes: * – points of the geodynamic GNSS network of FEB RAS/FEFU [*Bykov et al.*, 2020];
** – points of the PrinNet network of JSC "PRIN" (https://prinnet.ru/).

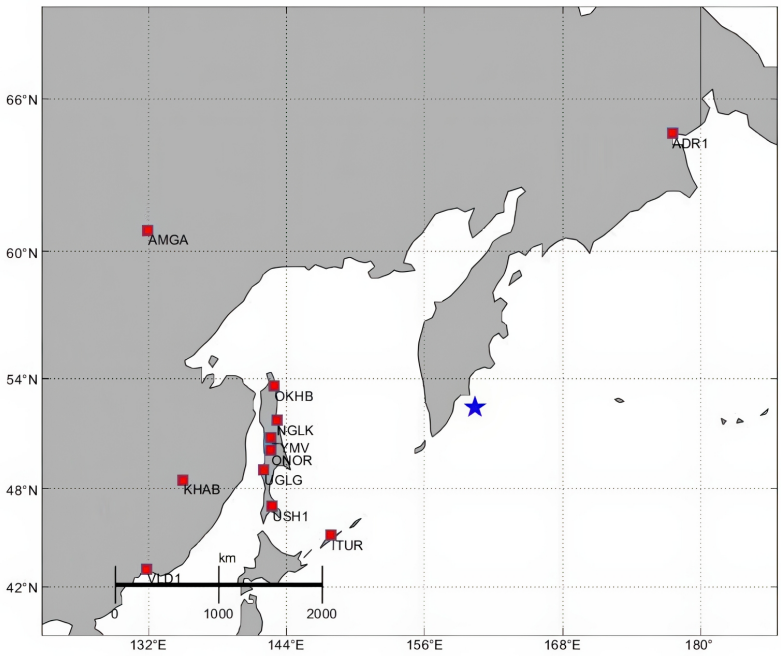

Figure 1. Locations of the GNSS observation points used for the waveform inversion of the Kamchatka earthquake on July 29, 2025. The earthquake's epicenter is marked with a star.

It is assumed that in the scale of the used instrumental networks the earthquake source can be approximated by a point source. In the case of an extended source, such as the earthquake on July 29, 2025, it is no longer possible to locate the CMT solution at the epicenter of the event, at least on a regional scale. The world agencies based on teleseismic records (GFZ, IPGP, USGS) continue to use the epicenter to search for CMT even for such significant events. ISOLA offers the ability to refine the centroid position by grid search.

For the event under study, it is tentatively assumed that the contact zone between the Pacific and Okhotsk lithospheric plates was ruptured along a deep-water trench across the entire depth of their contact (10–60 km). Therefore, it is logical to search for the centroid's position within the plate contact zone. The centroid depth was set to h = 30 km, which is

approximately half the depth of the plate contact zone. The position of the aftershock cloud in the days following the earthquake clearly shows that the origin is stretched southwest from the epicenter. Along the line with an azimuth of 214 degrees, parallel to the deep-water trough, 21 trial source positions were marked at 30 km intervals so that the epicenter of the earthquake (according to the Sakhalin branch of the FRC GS RAS – SAGSR agency code) was located above the fourth trial source position (Figure 2).

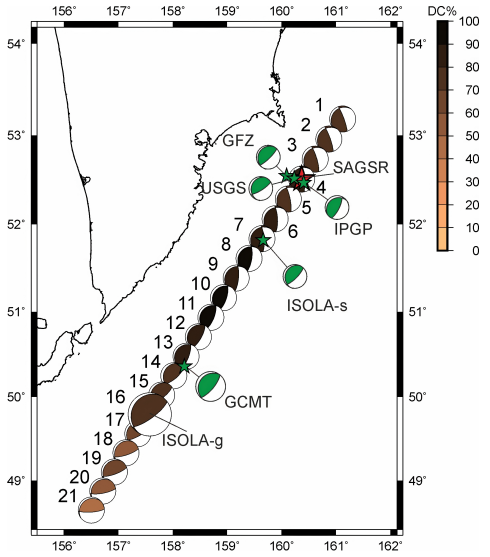

Figure 2. Position of earthquake sources relative to the coast of Kamchatka peninsula. Epicenter of Kamchatka earthquake on July 29, 2025 in accordance with SAGSR data is shown with a red star. Stereograms of the best solutions for each of the variants of centroid position are given, the optimum variant is the largest (ISOLA-g). The value of the DC component is shown by a color gradient from brown to black. The position (green stars) and stereograms of CMT solution variants of different agencies according to Table 1 are given.

During the inversion process, the centroid time was refined within a range of 0 to 240 seconds from the initial time t_0, with a step size of three seconds. Thus, 1890 possible centroid positions in space and time were considered.

The time function of the rupture was not specified separately. For weaker events, a delta function of zero duration is considered standard. Two approaches were tried for this event: a delta function and a 120-second triangle function. Both variants produced an identical solution, though the second case had a slightly larger seismic moment. However, the first variant produced a slightly more stable solution, so it was chosen as the primary one, despite being an obvious simplification.

The calculations were based on a one-dimensional velocity profile of the Earth's crust and mantle, which is well suited for the Kuril-Okhotsk region and Japan [*Kubo et al.*, 2002].

The same ISOLA settings were used to find a solution based on seismological data.

3. Results and Discussion

The optimal CMT solutions for the Kamchatka earthquake on July 29, 2025, based on seismological data and GNSS records, are presented in Table 1 under the names ISOLA-s and ISOLA-g, respectively. Figures 3 and 4 show the software's final report for the best solution based on seismological (Figure 3) and GNSS (Figure 4) data.

The quality of the solution obtained can be most clearly demonstrated by comparing real and synthetic waveforms. Figure 5 shows a comparison of waveforms for a solution based on GNSS records. The proximity of each pair of waveforms represents the variance reduction coefficient:

$$VR = 1 - \frac{|d-s|^2}{|d|^2},$$

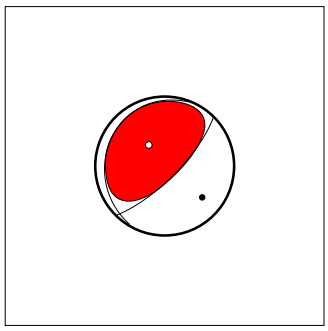

MOMENT TENSOR SOLUTION

HYPOCENTER LOCATION (SAGSR)

Origin time 20250729 23:24:51.00
Lat 52.51 Lon 160.37 Depth 56

Trial source number : 7 (Multiple Source line or plane inversion)
Centroid Lat (N)51.8372 Lon (E)159.6398
Centroid Depth (km) : 30
Centroid time : +72 (sec) relative to origin time

Moment (Nm) : 2.022e+22 Mw : 8.80
Inversion Type:Deviatoric
VOL% :0
DC% :80.3
CLVD% :19.7
Var.red.:(for stations used in inversion):0.79 NaN 9.5 47±26 0.44
Var.red.(for all stations) :

Strike Dip Rake | Frequency band used in inversion (Hz)
203 16 69 | 0.002 - 0.005
Strike Dip Rake |Stations-Components Used-Distance
45 75 96 | NS EW Z D(km)
|YSS - + + 1407
P-axis Azimuth Plunge |URH - + + 1637
130 30 |HSS + + + 1776
T-axis Azimuth Plunge |KHBR + + + 1841
323 59 |TMR + + + 1915
|MDJ + + + 2413
Mrr Mtt Mpp |HIA + + + 2843
1.079 -0.351 -0.728 |INCN + + + 3099
Mrt Mrp Mtp
1.298 1.176 -0.335
Exponent (Nm): 22

Figure 3. Results of the CMT calculation for the Kamchatka earthquake on July 29, 2025 by ISOLA software package using data from broadband seismometers (ISOLA-s).

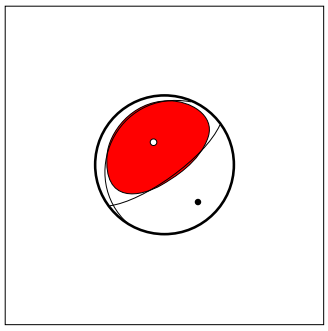

MOMENT TENSOR SOLUTION

HYPOCENTER LOCATION (SAGSR)

Origin time 20250729 23:24:51.00
Lat 52.51 Lon 160.37 Depth 56

Trial source number : 16 (Multiple Source line or plane inversion)
Centroid Lat (N)49.7927 Lon (E)157.5745
Centroid Depth (km) : 30
Centroid time : +123 (sec) relative to origin time

Moment (Nm) : 2.058e+22 Mw : 8.81
Inversion Type:Deviatoric
VOL% :0
DC% :72.2
CLVD% :27.8
Var.red.:(for stations used in inversion):0.59 NaN 8.6 36±22 0.15
Var.red.(for all stations) :

Strike Dip Rake | Frequency band used in inversion (Hz)
208 17 65 | 0.002 - 0.005
Strike Dip Rake |Stations-Components Used-Distance
54 74 97 | NS EW Z D(km)
|OKHB + + + 1172
P-axis Azimuth Plunge |NGLK + + + 1178
138 29 |ITUR + + + 1220
T-axis Azimuth Plunge |TYMV + + + 1234
334 60 |ONOR + + + 1257
|UGLG + + + 1342
Mrr Mtt Mpp |USH1 + + + 1407
1.207 -0.470 -0.737 |ADR1 + + + 1675
Mrt Mrp Mtp |KHAB + + + 1841
1.468 0.914 -0.364 |AMGA + + + 1952
Exponent (Nm): 22 |VLD1 + + + 2354

Figure 4. Result of the CMT calculation for the Kamchatka earthquake on July 29, 2025 by ISOLA software package using records of GNSS observation points (ISOLA-g).

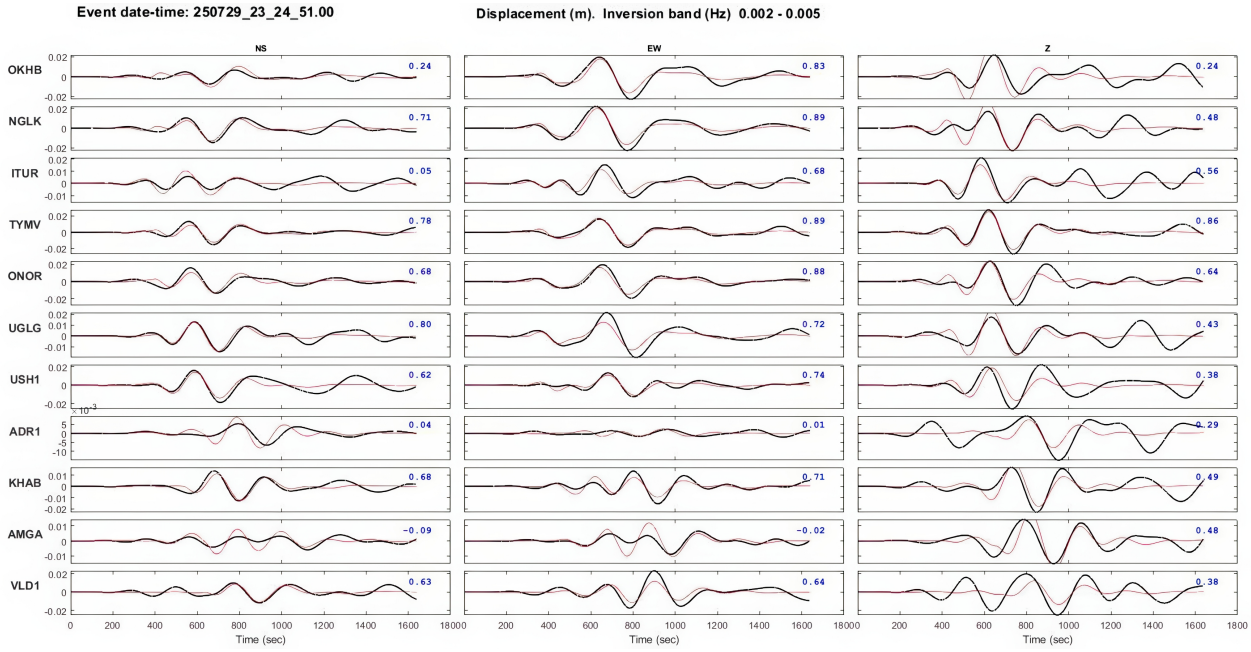

Figure 5. Comparison of real GNSS records of the Kamchatka earthquake on July 29, 2025 (black lines) and synthetic waveforms (red lines) in the filter band 0.002–0.005 Hz. Blue figures show the variance reduction factor.

where d and s are the instantaneous values of the real and synthetic records, respectively. In the case of perfect convergence of the records, this coefficient tends to 1; in the case of a mismatch, it decreases and can go far into negative values. Figure 5 shows the average VR coefficient for the channel in the upper right corner of each plot. The weighted average VR coefficient over all records serves as the main indicator of solution quality.

Figure 2 shows the best solutions for each possible position of the centroid in space. The optimal solution is at point #16, though variants 12 through 18 are quite close in terms of VR. It can be seen that both the position of nodal planes of the nearest double-couple (DC) solution varies significantly in neighboring trial sources, as well as the value of the DC-component of the solution, reflecting the closeness of the tensor to a pure DC-movement. Typically, the DC component of a tectonic earthquake is close to 100%, which serves as an indicator of a good solution. In Figure 2, we added the positions and variants of the beach balls of the main world agencies mentioned in Table 1, as well as the ISOLA-s variant obtained from seismological records. As can be seen, the ISOLA-g source mechanism solution variant based on GNSS data is quite close to the other variants. The centroid position is close to that obtained by GlobalCMT – the only agency in Table 1 that specified the event centroid position (the other agencies estimated the CMT at the epicenter). According to the finite-fault solutions for the July 29 earthquake [*USGS*, 2026], the maximum amplitudes of displacement along the seismic rupture were observed in this area. Notably, the ISOLA-s solution from seismological data, which is nearly identical in seismic moment tensor, is much farther northeast. This was probably a consequence of the poor azimuthal distribution of the seismic stations.

It is important to compare the seismic moment M_0 value of the ISOLA-g solution with those of other variants. As shown in Table 1, the USGS agency obtained the largest value of scalar seismic moment for the July 29 earthquake using the W-phase method, which is considered the most accurate for determining the seismic moment of mega-earthquakes. Three other agencies that used the full waveform method obtained smaller values of the scalar seismic moment. The scalar seismic moment of the ISOLA-s solution from seismic data was higher than those of the other agencies and was very close to the ISOLA-g solution. The influence of using only STS-1 records probably had an effect. Using GNSS data allowed us to obtain a value of M_0 that was closest to the USGS result. Consequently, the moment magnitude was $M_W = 8.81$, which was the least underestimated relative to the USGS data.

The CMT solution, in its double-couple approximation, is quite close to the variants listed in Table 1. The obtained variants, ISOLA-s and ISOLA-g, are intermediate between the variants of seismological agencies. There are many possible reasons for the discrepancy in the solutions, including the regional velocity section used, the azimuthal coverage, the use of only the closest observation points, the selection of such points from many variants, the choice of centroid position variants, and the approach to the time function used. The resulting solution type is a low-angle thrust fault with a shallow-dipping nodal plane to the northwest. Its coordinates correspond well with the orientation of the lithospheric plate boundary along which the displacement occurred during the Kamchatka earthquake on July 29, 2025.

4. Conclusion

This study demonstrates the possibility of determining the seismic moment tensor of a strong regional earthquake based on GNSS records using the ISOLA seismological software package.

The obtained solution corresponds well with solutions from other seismological agencies that used teleseismic broadband seismic station data and slightly exceeds the solution obtained using ISOLA and regional broadband seismic station records. This solution closely resembles the USGS "reference" solution obtained using the W-phase method. The refined centroid position is close to the GCMT centroid position and the maximum displacements along the seismic fault for the finite fault model.

In the Russian Far East and across Northeast Asia, GNSS networks provide a much wider selection of observational station displacement records than seismological stations equipped with broadband seismometers. In the case of the July 29, 2025, Kamchatka earthquake, the shortage of seismological records was exacerbated by the use of only Streckeisen STS-1 sensors and the clipping of records at stations closer than 1000 km from the epicenter. The large number of GNSS points enabled better azimuthal coverage and consequently better refinement of the centroid position. The absence of lower frequency limitations in GNSS records allowed us to determine the magnitude of the Kamchatka earthquake with high accuracy.

The use of real-time GNSS records of strong earthquakes in the region offers significant opportunities for the rapid and accurate determination of the focal parameters of strong and very strong, potentially tsunamigenic seismic events, which is critical for early warning of tsunami threats, wave propagation modeling, and the timely cancellation of tsunami warnings. The use of GNSS records in conjunction with traditional seismological data is advisable for inclusion in the operating procedures of seismological services responsible for recording regional earthquakes and warning populations in hazardous areas of the threat of a tsunami.

Acknowledgments. The work was carried out under the State Assignment of the IMGG FEB RAS. Work of N. V. Shestakov was partially supported by the state assignment for IAM FEB RAS No. 075-00460-26-00. The data used in the work were obtained with large-scale research facilities "Seismic infrasound array for monitoring Arctic cryolithozone and continuous seismic monitoring of the Russian Federation, neighboring territories and the world" (https://ckp-rf.ru/usu/507436/). The authors are grateful to JSC "PRIN" for providing data from the PrinNet GNSS network.

References

Abubakirov I. R., Gabsatarova I. P., Gileva N. A., et al. Focal mechanisms of selected earthquakes in Russia // Earthquakes in Russia in 2023. — Obninsk : GS RAS, 2025. — P. 217–226. — (In Russian).

Abubakirov I. R. and Pavlov V. M. Determining the Double Couple Moment Tensor for Kamchatka Earthquakes from Regional Seismic Waveforms // Izvestiya, Physics of the Solid Earth. — 2021. — Vol. 57, no. 3. — P. 332–347. — https://doi.org/10.1134/s1069351321030010

Bykov V. G., Shestakov N. V., Gerasimenko M. D., et al. Unified observation network for geodynamic monitoring in FEB RAS: formation, 10 years of development and major achievements // Vestnik of the FEB RAS. — 2020. — 3(211). — P. 5–24. — https://doi.org/10.37102/08697698.2020.211.3.001 — (In Russian).

Colosimo G., Crespi M. and Mazzoni A. Real-time GPS seismology with a stand-alone receiver: A preliminary feasibility demonstration // Journal of Geophysical Research: Solid Earth. — 2011. — Vol. 116, B11. — B11302. — https://doi.org/10.1029/2010jb007941

Crowell B. W., Melgar D., Bock Y., et al. Earthquake magnitude scaling using seismogeodetic data // Geophysical Research Letters. — 2013. — Vol. 40, no. 23. — P. 6089–6094. — https://doi.org/10.1002/2013GL058391

Davis P. Development and Operation of a Global-Scale Seismographic Network: The IRIS/USGS GSN // Perspectives of Earth and Space Scientists. — 2024. — Vol. 5, no. 1. — https://doi.org/10.1029/2023cn000225

Dziewonski A. M., Chou T. A. and Woodhouse J. H. Determination of earthquake source parameters from waveform data for studies of global and regional seismicity // Journal of Geophysical Research: Solid Earth. — 1981. — Vol. 86, B4. — P. 2825–2852. — https://doi.org/10.1029/jb086ib04p02825

Ekström G., Nettles M. and Dziewoński A. M. The global CMT project 2004-2010: Centroid-moment tensors for 13,017 earthquakes // Physics of the Earth and Planetary Interiors. — 2012. — Vol. 200/201. — P. 1–9. — https://doi.org/10.1016/j.pepi.2012.04.002

Gusman A. R., Tanioka Y., Sakai S., et al. Source model of the great 2011 Tohoku earthquake estimated from tsunami waveforms and crustal deformation data // Earth and Planetary Science Letters. — 2012. — Vol. 341–344. — P. 234–242. — https://doi.org/10.1016/j.epsl.2012.06.006

Hayes G. P., Rivera L. and Kanamori H. Source Inversion of the W-Phase: Real-time Implementation and Extension to Low Magnitudes // Seismological Research Letters. — 2009. — Vol. 80, no. 5. — P. 817–822. — https://doi.org/10.1785/gssrl.80.5.817

Käufl P., Valentine A. P., O'Toole T. B., et al. A framework for fast probabilistic centroid-moment-tensor determination-inversion of regional static displacement measurements // Geophysical Journal International. — 2014. — Vol. 196, no. 3. — P. 1676–1693. — https://doi.org/10.1093/gji/ggt473

Kostylev D. V. Formation of a unified system for collecting seismological information in the Sakhalin Division GS RAS // Russian Journal of Seismology. — 2021. — Mar. — Vol. 3, no. 1. — P. 41–53. — https://doi.org/10.35540/2686-7907.2021.1.03 — (In Russian).

Kubo A., Fukuyama E., Kawai H., et al. NIED seismic moment tensor catalogue for regional earthquakes around Japan: quality test and application // Tectonophysics. — 2002. — Vol. 356, no. 1–3. — P. 23–48. — https://doi.org/10.1016/s0040-1951(02)00375-x

Melgar D., Bock Y. and Crowell B. W. Real-time centroid moment tensor determination for large earthquakes from local and regional displacement records // Geophysical Journal International. — 2012. — Vol. 188, no. 2. — P. 703–718. — https://doi.org/10.1111/j.1365-246X.2011.05297.x

Melgar D., Crowell B. W., Geng J., et al. Earthquake magnitude calculation without saturation from the scaling of peak ground displacement // Geophysical Research Letters. — 2015. — Vol. 42, no. 13. — P. 5197–5205. — https://doi.org/10.1002/2015gl064278

O'Toole T. B., Valentine A. P. and Woodhouse J. H. Centroid-moment tensor inversions using high-rate GPS waveforms: CMT inversions using high-rate GPS waveforms // Geophysical Journal International. — 2012. — Vol. 191, no. 1. — P. 257–270. — https://doi.org/10.1111/j.1365-246x.2012.05608.x

Quinteros J., Strollo A., Evans P. L., et al. The GEOFON Program in 2020 // Seismological Research Letters. — 2021. — Vol. 92, no. 3. — P. 1610–1622. — https://doi.org/10.1785/0220200415

Riquelme S., Bravo F., Melgar D., et al. W phase source inversion using high-rate regional GPS data for large earthquakes // Geophysical Research Letters. — 2016. — Vol. 43, no. 7. — P. 3178–3185. — https://doi.org/10.1002/2016GL068302

Safonov D. A. and Konovalov A. V. Moment tensor inversion in the Kuril-Okhotsk and Sakhalin Regions using ISOLA software // Tikhookeanskaya geologiya. — 2017. — Vol. 36, no. 3. — P. 102–112. — (In Russian).

Safonov D. A., Konovalov A. V. and Zlobin T. K. The Urup earthquake sequence of 2012-2013 // Journal of Volcanology and Seismology. — 2015. — Vol. 9, no. 6. — P. 402–411. — https://doi.org/10.1134/s074204631506007x

Sokos E. and Zahradnik J. Evaluating Centroid-Moment-Tensor Uncertainty in the New Version of ISOLA Software // Seismological Research Letters. — 2013. — Vol. 84, no. 4. — P. 656–665. — https://doi.org/10.1785/0220130002

Sokos E. N. and Zahradnik J. ISOLA a Fortran code and a Matlab GUI to perform multiple-point source inversion of seismic data // Computers & Geosciences. — 2008. — Vol. 34, no. 8. — P. 967–977. — https://doi.org/10.1016/j.cageo.2007.07.005

Trabant C., Hutko A. R., Bahavar M., et al. Data Products at the IRIS DMC: Stepping Stones for Research and Other Applications // Seismological Research Letters. — 2012. — Vol. 83, no. 5. — P. 846–854. — https://doi.org/10.1785/0220120032

USGS. M 8.8 - 2025 Kamchatka Peninsula, Russia Earthquake. Finite Fault. — 2026. — URL: https://earthquake.usgs.gov/earthquakes/eventpage/us6000qw60/finite-fault (visited on 01/26/2026).

Vallée M. and Douet V. A new database of source time functions (STFs) extracted from the SCARDEC method // Physics of the Earth and Planetary Interiors. — 2016. — Vol. 257. — P. 149–157. — https://doi.org/10.1016/j.pepi.2016.05.012

Zahradnik J., Serpetsidaki A., Sokos E., et al. Iterative Deconvolution of Regional Waveforms and a Double-Event Interpretation of the 2003 Lefkada Earthquake, Greece // Bulletin of the Seismological Society of America. — 2005. — Vol. 95, no. 1. — P. 159–172. — https://doi.org/10.1785/0120040035

Zheng Y., Li J., Xie Z., et al. 5Hz GPS seismology of the El Mayor-Cucapah earthquake: estimating the earthquake focal mechanism // Geophysical Journal International. — 2012. — Vol. 190, no. 3. — P. 1723–1732. — https://doi.org/10.1111/j.1365-246x.2012.05576.x